PEEL ZONE MODEL OF TAPE PEELING BASED ON THE GECKO ADHESIVE SYSTEM

N. S. Pesika[*], Y. Tian, B. Zhao, K. Rosenberg, H. Zeng, P. McGuiggan, and J. N. Israelachvili
Department of Chemical Engineering, University of California
Santa Barbara, CA 93106

K. Autumn
Department of Biology, Lewis and Clark College
Portland, OR 97129

ABSTRACT

A tape peeling model based on the geometry of the peel zone (PZ) is derived to predict the peeling behavior of adhesive tapes at peel angles less than or equal to 90°. The PZ model adds an angle-dependent multiplier to the 'Kendall equation' that takes into account the geometrical changes within the peel zone. The model is compared to experimental measurements of the peel force at different angles for a model tape and two commercial tapes, each with different bending moduli, stretch moduli and adhesive strengths. Good agreement is found for a wide range of peel angles. The PZ model is also applied to the gecko adhesive system and predicts a spatula peel angle of 18.4° to achieve the adhesion forces reported for single setae. The PZ model captures the fact that *adhesive* forces can be significantly enhanced by peeling at an angle, thereby exploiting high *friction* forces between the detaching material and the substrate.

1.   INTRODUCTION

Understanding how geckos derive a high adhesion and friction force from their adhesive pads, and the role of geometry, is essential for the design of dry adhesives. Autumn et al. [Autumn et al., 2000; Autumn et al., 2002] were the first to show that the relatively weak van der Waals forces are responsible for strong gecko adhesion. This is due to the complex hierarchical structure (geometry) of the gecko, coupled to the compliances of the different components of the adhesive system [Yao and Gao, 2006], which allows for intimate contact of the adhesive pads to almost any surface. In addition, the way these hierarchical structures are articulated (e.g., their configuration and angles at which they are pulled, shown in Fig. 1A) result in large adhesion forces $F_\perp$ acting normal to the surface. The fact that van der Waals forces are always present between any two surfaces in contact has motivated the fabrication of dry adhesives inspired by the gecko adhesive system [Geim et al., 2003; Northen and Turner, 2005]. Geckos further enhance the adhesion of the adhesive pads by exploiting the high friction forces $F_\parallel$– again due to van der Waals forces- acting parallel to the surface. The biomechanics of a gecko walking on a surface [Chen et al., 2006;

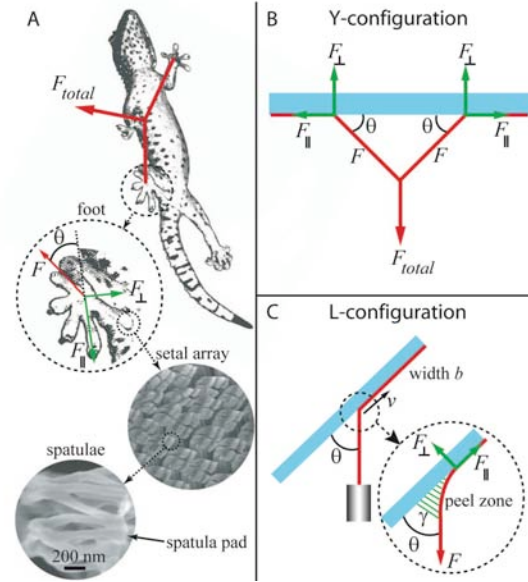Fig. 1. (A) Ventral view of a gecko walking on a glass surface. Each toe is composed of a hierarchical level of structures; the setae (approximately 100 μm in length x 5 μm in diameter keratin-based pillars which originate from the gecko toe skin and split into 100-1000 spatulae (triangular keratin-based adhesive structures that make up the final hierarchical level of the gecko adhesive system structures. They are approximately 200 nm at the base narrowing to ~100 nm and 10 nm in thickness)) (B) Schematic of the 'Y-configuration' showing a force balance between the tape and the surface (C) Schematic of the 'L-configuration' used in peel tests showing the different forces in the peel zone.

Autumn et al., 2006a] reveals the use of a particular configuration, referred to here as the 'Y-configuration' (Figure 1B). In this configuration, to make a step forward, the gecko always has two diagonally opposite feet on the surface while detaching the other two, as shown in Figure 1A. The two attached feet (front right and back left feet in Figure 1A) are angled to the surface at an angle θ with a tension F along the feet, making a Y-shaped geometry and yielding a total force $F_{total}=2\,F_\perp$ in the normal direction to the surface. The Y-shaped geometry was also reported by Autumn et al. [Autumn et al., 2006b] in which it was found that the opposing feet

Report Documentation Page

1. REPORT DATE **01 NOV 2006**	2. REPORT TYPE **N/A**	3. DATES COVERED **-**

4. TITLE AND SUBTITLE **Peel Zone Model of Tape Peeling based on the Gecko Adhesive System**	5a. CONTRACT NUMBER
	5b. GRANT NUMBER
	5c. PROGRAM ELEMENT NUMBER
6. AUTHOR(S)	5d. PROJECT NUMBER
	5e. TASK NUMBER
	5f. WORK UNIT NUMBER
7. PERFORMING ORGANIZATION NAME(S) AND ADDRESS(ES) **Department of Chemical Engineering, University of California Santa Barbara, CA 93106**	8. PERFORMING ORGANIZATION REPORT NUMBER
9. SPONSORING/MONITORING AGENCY NAME(S) AND ADDRESS(ES)	10. SPONSOR/MONITOR'S ACRONYM(S)
	11. SPONSOR/MONITOR'S REPORT NUMBER(S)

12. DISTRIBUTION/AVAILABILITY STATEMENT **Approved for public release, distribution unlimited**

13. SUPPLEMENTARY NOTES **See also ADM002075., The original document contains color images.**

14. ABSTRACT

15. SUBJECT TERMS

16. SECURITY CLASSIFICATION OF:			17. LIMITATION OF ABSTRACT **UU**	18. NUMBER OF PAGES **24**	19a. NAME OF RESPONSIBLE PERSON
a. REPORT **unclassified**	b. ABSTRACT **unclassified**	c. THIS PAGE **unclassified**			

of the gecko were pulling inwards towards the centre of mass. The peel test schematically shown in Figure 1C, referred to here as the 'L-configuration', is a common test used to characterize the peeling behavior of adhesive tapes and was used here to study the gecko adhesive system while the animal is at rest or in motion.

Many complex models have been proposed to describe the peeling behavior of adhesive tapes [Rivlin, 1944; Kendall, 1975; Gent and Kaang, 1987; Kinloch et al., 1994; Wan, 1999; Plaut and Ritchie, 2004; Sato and Toda, 2004; Sun et al., 2004; Williams and Kauzlarich, 2005]. One of the most commonly used models was first proposed by Rivlin [Rivlin, 1944] and modified by Kendall [Kendall, 1975] to include the elastic energy of the tape backing. The Kendall equation, Equation (1), originally applied to the detachment of a thin elastomeric film from a rigid surface, is widely used and has been confirmed by numerous experiments [Ciccotti et al., 2004; Newby and Chaudhury, 1998]. Previous studies of gecko adhesion [Persson and Gorb, 2004; Spolenak et al., 2004; Huber et al., 2005; Hansen and Autumn 2005] have modeled the adhesive pads of geckos as nanoscale strips of tape. For the geometry shown in Figure 1C, the Kendall equation for the peel force is [Kendall, 1975]:

$$\frac{F}{b} = \frac{\gamma}{(1 - \cos\theta)} + \text{elastic energy term} \qquad [1]$$

where F is the peel force in the peeling direction, b is the tape width, γ is the crack energy and θ is the peel angle. The Kendall equation (neglecting the elastic energy term of the tape backing) is derived based on an energy balance by considering the adhesive force between the tape and the surface and the amount of energy required to peel the tape to a new location while at a constant peel angle θ. The Kendall equation inherently does not provide any information about the geometry of the peel zone nor how friction forces contribute to the adhesion force.

In previous work [Tian et al., 2006], we performed a molecular level analysis to estimate the pulling force generated by the adhesion and friction of a single spatula by considering van der Waals forces between the adhering surfaces. In this paper, we use a macroscopic analysis, i.e., tape peeling, to model the adhesion of a single gecko spatula.

2. THEORY

We derive a new quantitative model for tape peeling based on the geometry of the peel zone (PZ model), as ascertained from microscopic observations of the peel zone during detachment, as described later. The PZ model is derived based on a force balance at the peel zone and takes into account three forces: the peel force F

Fig. 2. Schematic illustration of the peel zone showing the two peel regimes: constant peel zone regime and variable peel zone regime.

acting in the peel direction, the adhesion force $F_\perp$ acting normal to the surface, and the friction/shear force $F_\parallel$ acting parallel to the surface. The peel zone is defined as the bifurcation between the tape backing and the surface in which cavitation and fibrillation occur (Figure 1C) [Zosel, 1989; Zosel, 1998; Créton and Leibler, 1996; Lindner et al., 2004; Shull et al., 2004; Portigliatti et al., 2000]. We assume that the curvature of the tape backing is circular and that the length of the peel zone on the surface is equal to the arc length of the tape backing up to the point of the last fibril or filament. We also assume that the tape is composed of a backing material that has a large stretch modulus, i.e., the tape does not stretch significantly. As the peel angle gets smaller, a larger fraction of the peel force F is opposed by the friction/shear force $F_\parallel$ provided by the surface. The friction force "pins" the contact end of the peel zone (using a Lagrangian reference coordinate system that moves at the same velocity v as the peel front) thereby increasing the radius of curvature R of the tape backing as shown later in Figure 2 and described by Equation (11). The increased radius of curvature R increases the length of the peel zone, which in turn increases the peel force F in the peel direction θ. We do not consider the variation of the filament strengths as a function of the filament lengths in this model, but instead assume that the peel zone provides an average adhesive tensile force. Figure 2 shows a schematic of the peel zone for two cases: peel angles between the red and blue solid lines (constant peel zone regime), and between the blue and brown solid lines (variable peel zone regime). In the 'constant peel zone regime', the geometry of the peel zone, i.e., the length of the peel zone and the curvature of the tape backing, remains constant while the peel angle θ is changed. In contrast, in the 'variable peel zone regime', the length of the peel zone and the curvature of

the tape baking both increase as the peel angle θ is changed. The peel zone region is bounded by the 'leading edge' and the 'stationary point' (the location of the last active filament). The stationary point is assumed to remain at the same normal distance from the detaching surface for all peel angles since it is determined by the (constant) tensile force of the last active filament. The normal component of the peel force $F_\perp$ is proportional to the area of the peel zone,

$$F_\perp \propto Sb, \text{ or } F_\perp = CSb, \qquad [2]$$

where S is the length of the peel zone, b is the width of the tape, and C is a constant multiplier. The crack energy γ of the tape detachment is defined for a 90° peel angle for which the length of the peel zone is S_o, where

$$\frac{F_\perp}{b} = \gamma = CS_o, \qquad [3]$$

so that

$$C = \frac{\gamma}{S_o}. \qquad [4]$$

Solving and substituting the constant C into Equation (2) gives the normal peel force per unit width of tape:

$$\frac{F_\perp}{b} = CS = \frac{\gamma}{S_o}S. \qquad [5]$$

The total peel force per unit width of tape F/b as a function of the peel angle θ is therefore $\dfrac{F}{b} = \dfrac{F_\perp}{b\sin\theta}$.

2.1 Constant Peel zone detachment mode

For a tape backing with a finite bending modulus E, the last active filament spans an angle ϕ_o along the tape backing (Figure 2). Depending of the tackiness of the adhesive [Zosel, 1989; Zosel, 1998; Créton and Leibler, 1996; Lindner et al., 2004; Shull et al., 2004; Portigliatti et al., 2000], ϕ_o can range from 90° (large tackiness) to almost 0° (small tackiness). For peel angles greater than ϕ_o, the shape and dimension of the peel zone remains constant and thus the normal component of the peel force also remains constant. In this case, Equation (5) reduces to $\dfrac{F_\perp}{b} = \gamma$, and the peel force per unit width of tape reduces to

$$\frac{F}{b} = \frac{\gamma}{\sin\theta}. \qquad [6]$$

Alternatively, Equation (6) can be derived by considering a force balance at the peel zone. As shown in Figure 1C, the peel force F at a peel angle θ is balanced by contributions from the adhesion component $F_\perp$ and the friction/shear component $F_\parallel$, which are related by

$$F = F_\perp \sin\theta + F_\parallel \cos\theta. \qquad [7]$$

In addition, the relationship between the adhesion and friction/shear components is: $\tan\theta = \dfrac{F_\perp}{F_\parallel}$. Substituting the latter into Equation (7) yields:

$$F = \frac{F_\perp}{\sin\theta}, \qquad [8]$$

which when combined with Equation (3) gives Equation (6).

2.2 Variable Peel zone detachment mode

As the peel angle θ approaches ϕ_o, the shape and dimension of the peel zone changes gradually from the constant peel zone detachment mode to the variable peel zone detachment mode. Here we assume that this change occurs abruptly when the peel angle reaches ϕ_o. At this point, the length of the peel zone is given by:

$$S_o = R_o\phi_o, \qquad [9]$$

where R_o is the radius of curvature of the tape backing at $\theta = \phi_o$. As the peel angle decreases further, the new length of the peel zone changes to

$$S = R\theta, \text{ where } \theta < \phi_o, \qquad [10]$$

and where R is the new radius of curvature of the tape backing at the peel angle θ. Using simple trigonometric relationships, it can be shown that

$$\frac{R}{R_o} = \frac{1 - \cos\phi_o}{1 - \cos\theta}. \qquad [11]$$

Substituting the above relationship into Equation (5), the peel force for the variable peel zone detachment mode is given by

$$\frac{F(\theta, \phi_o)}{b} = \gamma \left[\frac{\theta}{\phi_o}\right]\left[\frac{1 - \cos\phi_o}{1 - \cos\theta}\right]\left[\frac{1}{\sin\theta}\right]. \qquad [12]$$

The reference crack energy γ is defined when $\theta = \phi_o$. In this case, Equation (12) reduces to

3

$$\frac{F}{b} = \frac{\gamma}{\sin\phi_o}. \qquad [13]$$

Solving for γ yields:

$$\gamma = \frac{F\sin\phi_o}{b}. \qquad [14]$$

In the special case in which the tape backing is sufficiently compliant and the curvature of the backing is dictated solely by the adhesive layer (for example, an adhesive with high tack), $\phi_o = 90°$ and Equation (12) reduces to

$$\frac{F}{b} = \frac{2\gamma\theta}{\pi(1-\cos\theta)\sin\theta}, \qquad [15]$$

and the reference crack energy defined at $\theta = \phi_o = 90°$ peel is now given by

$$\gamma = \frac{F}{b}. \qquad [16]$$

The PZ model differs from the 'Kendall equation' (cf Equations (12) and (1)) by an angle-dependent multiplier, which takes into account the increase in the length of the peel zone S as the peel angle is reduced. This factor causes the peel force predicted by the PZ model to be always smaller than the value given by the 'Kendall equation', the largest difference occurring at smaller peel angles.

3. EXPERIMENTAL

A model tape was created by using a double-sided tacky adhesive transfer tape (3M #950 – 0.13 mm adhesive thickness) as the adhesive layer, and a transparency sheet (3M Write-on Transparency film – 0.1 mm in thickness) as the stiff tape backing. The transfer tape was adhered to the transparency sheet using a hand-roller (4.5 lb, ChemInstruments Inc.). To ensure maximum adhesion between the transparency film and the transfer tape, the model tape was not used until the following day. The model tape was then cut into 1/4-inch wide and 12-inch long strips. A glass surface (Borosilicate 1/4 inch x12 inch x6 inch, McMaster-Carr) was used as the substrate surface in the peeling test. The surface was cleaned 3 times with diacetone alcohol (purity 99%, Sigma Aldrich) followed by 3 times with acetone (ACS grade, EMD) using Kimwipes (Kimtech science) between each cleaning to remove the solvent. All chemicals were used as received. In addition, two commercial adhesives tapes, 3M Scotch[TM] tape (3/4 inch) and 3M Electrical tape (3/4 inch) were used in this study.

The 12-inch long strips of tape were attached to the glass surface using a rolling cylinder to prevent entrapment of air between the glass and adhesive. A 4.5 lb hand-roller was then used three times in each direction to ensure complete and uniform contact between the adhesive tape and glass. Peeling experiments were started after 1 hr and 4 hrs of allowing the tape to be in contact with the glass at room temperature (23 °C) for the model tape and commercial tapes, respectively. A schematic of the experimental set-up is shown in Figure 1C. The glass surface was positioned at a predetermined angle θ and the peel force F was varied (using brass weights) to attain a desired tape detachment velocity v of approximately 0.03 mm/s for the model tape and 0.5 mm/s for the commercial tapes. In each experiment using the commercial tapes, the tape was allowed to reach a steady detachment velocity v (typically after ~1 cm of peeling) before v was measured. Videos of the model tape peeling during the experiments were obtained using a monochrome camera (Pulnix) with a 10x objective. Still images were obtained from the videos and image processing (Adobe Photoshop) was performed to obtain the well-defined edges found in Figure 4. All experiments were run under ambient humidity and temperatures between 23 and 24°C.

4. RESULTS AND DISCUSSION

Since the transfer tape used to create the model tape is tacky, it allowed for the formation and visualization of relatively long filaments in the peel zone. Although the tape backing was relatively thick (0.1 mm thick transparency film), which increased the bending modulus E, the high adhesive strength of the transfer tape still determined the curvature of the tape and backing. In addition, the backing had a high stretch modulus, which is a pre-requisite for the model and is also a relevant model system for the gecko adhesive system since the spatula pads in geckos are composed of β-keratin, which is very stiff with a Young's modulus of approximately 1.5 GPa [Autumn et al, 2006c]. The last active filament of the transfer tape spans an angle of $\phi_o \approx 90°$, as shown in Figure 3A. Figure 3B shows a plot of the measured peel force for the detachment of the model tape from the borosilicate glass surface as a function of the peel angle θ in the range 30°-90°. Using Equation (12) for $\phi_o = 90°$, the model (solid line) accurately predicts the peeling behavior of the tape within the range of angles studied. The crack energy γ, defined at $\theta = 90°$, is 519 Nm^{-1} as determined by Equation (14). The reported value for the adhesion strength of the same transfer tape to steel is 820 Nm^{-1}. Note that the crack energy γ is not equal to the thermodynamic surface energy and is both substrate and detachment velocity v dependent. For comparison, the Kendall equation, Equation (1), is also shown in Figure 3 (dashed line) using the same crack energy of 519 Nm^{-1} since the crack energy used in the Kendall equation is
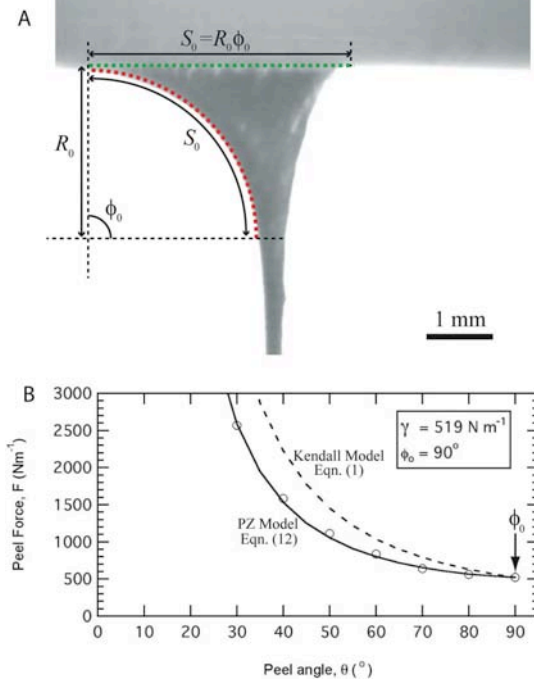
4

Fig. 3. (A) Optical image of a 90° peel of the model tape. The solid lines represent the predictions of the model for the curvature (dotted red curve) of the backing and the length of the peel zone (dotted green line). (B) Plots of measured and theoretical peel forces versus peel angle for a model tape consisting of a transfer tape adhesive on a transparency film backing at a peel velocity of $v\sim$ 0.03 mm/s. The solid line is the prediction of Equation (12). The dashed line is the prediction of Equation (1). In both cases, a crack energy of 519 Nm^{-1} was used as defined at ϕ_o=90°.

defined for a peel angle θ=90°. Although the model does predict the correct trend, it increasingly overestimates the peel force as the peel angle decreases.

In addition to predicting the peel force curve, the model is also capable of predicting the change in the curvature of the backing radius R and the length of the peel zone S as a function of the peel angle θ. Snap shot images of the peeling model tape from the borosilicate glass surface at various peel angles θ are shown in Figure 4. The dotted red curves and the dotted green lines represent the predictions for the curvatures, using Equation (11), and the lengths of the peel zones, using Equation (10), respectively, both showing good agreement with the recorded images. The small variations in the lengths of the peel zone are a consequence of the chaotic nature of the adhesive rupture of the filaments from the glass surface, whereas the model predicts the mean (or average) length of the peel zone.

Figure 5A shows an optical image of a composite tape consisting of a layer of 3M Electrical tape in
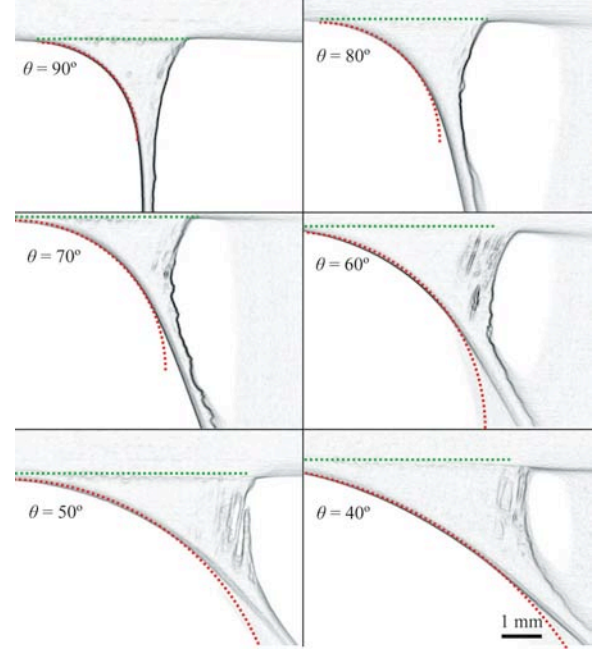
Fig. 4. Optical images of the peel zone region of the model tape peeling at a velocity of $v\sim$0.03 mm/s at peel angles of θ = 90°, 80°, 70°, 60°, 50° and 40°. The corresponding model predictions for the curvature (dotted red curves) and the length of the peel zone (dotted green lines) are superimposed on the optical images.

addition to a layer of 3M Scotch^{TM} tape peeling at θ=90°. The curvature of the backing R_o was measured to be 415 μm (dotted red Line). The active length in the peel zone S_o is 470 μm (dotted green line). Based on the active length of the peel zone and the curvature of the backing, ϕ_o was calculated to be 65° using Equation (9). Figure 5B is a plot of the peel force versus peel angle for the detachment of the tapes. A single layer of electrical tape has a low stretching modulus i.e., the tape elongates substantially even under a small tension. Thus the model, Equation (12), (solid curve in Figure 5B) is unable to correctly predict the peeling behavior of the tape at peel angles less than about 70° (✕ data points in Figure 5B). To overcome this issue, a second layer of 3M Scotch^{TM} tape was added over the electrical tape. This modification increases the stretching modulus of the composite tape while maintaining the adhesive properties of the electrical tape unchanged. Using Equation (12) with ϕ_o=65°, the model correctly predicts the peeling behavior of the composite tape for angles as low as 30° (○ data points in Figure 5B). At even smaller angles, substantial stretching of the tape occurred due to the high loads applied. The crack energy, as calculated from Equation (14), gives a value of 270 Nm^{-1} defined at θ =65°.

Figure 6A shows an optical image of a composite tape consisting of two layers of 3M Scotch^{TM} tape

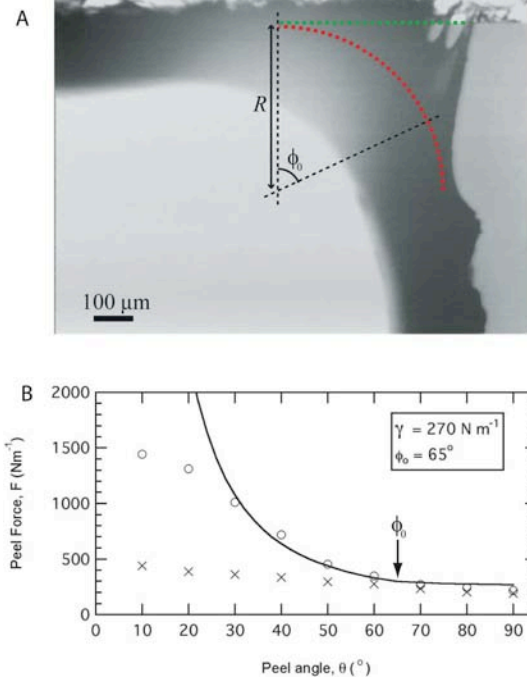Fig. 5. (A) Optical image of a 90° peel of a composite tape composed of a layer of 3M Electrical tape with an additional later of 3M Scotch^{TM} tape. (B) Plots of measured and theoretical peel forces versus peel angle for 3M electrical tape for a peel velocity of $v\sim0.5$ mm/s. The solid line is the prediction of Equation (15). ($\times$ – data for a single layer of tape, $\bigcirc$ – data for the composite tape)

Fig. 6. (A) Optical image of a 90° peel of the composite tape composed of two layers of 3M Scotch^{TM} tape. (B) Plots of measured and theoretical peel forces versus peel angle for 3M Scotch^{TM} tape for a peel velocity of $v\sim0.5$ mm/s. The solid line is the prediction of Equation [15]. ($\times$ – data for a single layer of 3M Scotch^{TM} tape, $\bigcirc$ – data for the composite tape)

peeling at θ=90°. The value for ϕ_o was again determined from the length of the peel zone and the radius of curvature of the tape. Figure 6B is a plot of the peel force versus peel angle for the detachments of a single and double layers of 3M Scotch^{TM} tape. A single layer of 3M Scotch^{TM} tape has a relatively high stretch modulus, and the model correctly predicts the peeling behavior for angles larger than 40°. Again, at lower peel angles, significant stretching of the tape occurs. By applying a second layer of 3M Scotch^{TM} tape, the stretching is diminished and again the agreement with Equation (12) with ϕ_o=62° is better, now down to $\theta\approx$20°. The crack energy, as calculated from Equation (14), gives a value of 181 Nm^{-1} defined at θ =62°.

4.1 Application of the model to the gecko adhesive system

Our model is particularly suited for application to the adhesion of geckos on surfaces due to the high elastic modulus of the keratin adhesive 'backing' structures in the gecko: the setae and spatulae, and generally low peel angles. However, the small dimensions of gecko setae and spatulae make their forces and geometry difficult to study. Huber et al. [Huber et al., 2005] measured the maximum pull-off force for a single spatula to be approximately 10 nN. If each spatula on a seta can generate 10 nN, it would take approximately 4000 spatulas to generate the adhesion force of 40 μN reported by Autumn et al. [Autumn et al, 2002] for a single seta. But, a seta contains a maximum of approximately only 1000 spatulas [Ruibal and Ernst, 1965], which would give 40 nN per spatula (a factor of 4 greater than obtained by Huber et al.). This apparent inconsistency in the forces measured on a single spatula compared to a single seta may be due to the different methods used to measure the adhesion forces. Huber et al. measured the pull-off force of a spatula by pulling the seta perpendicularly from a surface, which is an analog to tape peeling at 90° at the spatula level. On the other hand, Autumn et al. measured the pull-off force of a seta (containing multiple spatulas) by shearing the seta as well as applying a normal force away from the surface. According to our model, the friction force produced by shearing the seta would increase the peel zone of individual spatulas, thus increasing their adhesion force. Assuming that the van der Waals forces dictate the curvature of the spatula (i.e., the spatula is compliant), we can take $\phi_o\approx$90°. Using Equation (12) with a crack energy γ of 50 mNm^{-1} and ϕ_o=90° (obtained by using Equation (14) with F =10 nN reported by Huber et al. and the width of a spatula b = 200 nm), we obtain a peel force curve for a single spatula shown in Figure 7 (solid

6

curve). The crack energy in this case is set closer to the thermodynamic surface energy due to the lack of viscoelastic adhesive fibers present in pressure sensitive tapes. The peel angle θ required to yield 40 nN of normal adhesion force $F_\perp$ (equivalent to a peel force F of about 633 mNm^{-1}) per spatula is found to be approximately 18.4°. Also shown in Figure 7 is a plot of the adhesion force calculated in our previous work [Tian et al., 2006] using a molecular level analysis (dotted curve) by considering van der Waals forces between a spatula and a surface. Since typical values were used in the molecular level analysis, the magnitude of the peel force calculated is offset to larger values although the analysis does predict a similar trend to that predicted by the PZ model. By multiplying the values obtained by Tian et al. [Tian et al., 2006] by a fitting factor of 0.55, we find a good agreement between the molecular level analysis and the PZ model for the peel force of a single spatula (dashed curve).

At a peel angle of 18.4°, the component of the peel force acting parallel to the substrate (i.e., the friction force) is,

$$F_\parallel = \frac{F_\perp}{\tan\theta} = \frac{40\text{ nN}}{\tan 18.4°} = 120\text{ nN}. \qquad [17]$$

The maximum *available* friction force $F_\parallel^{available}$ is defined as the point at which the adhering surface begins to slip i.e., the parallel component of the peel force is greater than the friction that can be provided by the adhering surfaces. $F_\parallel^{available}$ is proportional to 3 different normal force contributions but can be approximated as follows:

$$F_\parallel^{available} = \mu\left(F_\perp^{balanced} + F_\perp + L\right) \approx \mu F_\perp^{balanced} \quad [18]$$

where μ is the coefficient of friction, $F_\perp^{balanced}$ is the *balanced* normal force (i.e., the balanced adhesion force between the spatula and the surface), and L is the applied normal load. Contribution from $F_\perp$ and L (±weight of a gecko spread over all the spatulae pads depending whether it is on the ground or on the ceiling) are negligible compared to $F_\perp^{balanced}$. The latter can be estimated by the van der Waals force between two flat surfaces [Israelachvili, 2005, chapter 11] as

$$F_\perp^{balanced} = \frac{AC_{spatula}}{6\pi D^3}, \qquad [19]$$

where A is the Hamaker constant, $C_{spatula}$ is the true contact area between the spatula and the surface, and D is the distance between the spatula and the surface. Taking $A=1\times10^{-19}$ J and $D=0.2$ nm as typical values [Israelachvili, 2005, chapter 11], and $C_{spatula}= 4\times10^{-14}$ m^2 (spatulae pads are ~200 nm in length and width),
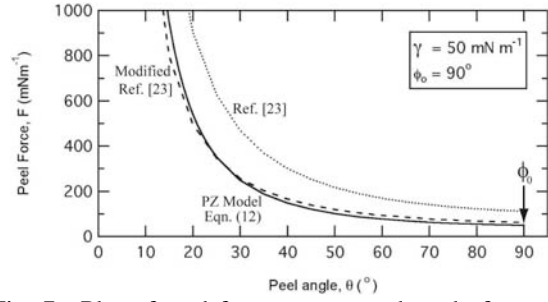

Fig. 7. Plot of peel force versus peel angle for a single spatula as given by Equation (12) using a crack energy of 50 mN m^{-1} as obtained by Huber et al. [Huber et al., 2005] and ϕ_o=90°. The dotted curve is the peel force of a single spatula as a function of peel angle obtained from reference [Tian et al, 2006]. The dashed curve is a fit of the peel force obtained from reference [Tian et al, 2006].

$F_\perp^{balanced} \approx 26$ mN. Assuming a friction coefficient of 0.25 between the spatulae pads and surface [Autumn et al., 2006b], $F_\parallel^{available} \approx 6.6$ mN. The available friction force is greater by over an order of magnitude than the required $F_\parallel = 120$ nN to sustain the peel force at 18.4°. This peel angle is also consistent with the 'frictional adhesion' model proposed by Autumn et al. [Autumn et al., 2006b], which states that $F_\parallel \geq -\dfrac{F_\perp}{\tan\alpha^*}$ where α^* is the critical detachment angle of the setae. For $\alpha^* = 30^o$, $1/\tan\alpha^* = 1.7$. In our case, the shear component $F_\parallel$ is 3 times (1/tan 18.4°) greater than the adhesion component $F_\perp$ of the peel force.

A limitation of the current model is that it is unable to predict the peeling behavior of tapes with small stretch moduli or at very low peel angles, where significant stretching occurs due to the large peel forces. The stretching of the backing is expected to decrease the length of the peel zone due to filament rupture within the peel zone. But in the case of the gecko adhesive system, instead of adhesive filaments dictating the curvature of a compliant backing and the adhesive force, van der Waals forces act on the spatula, so that stretching of the spatulae is not expected to significantly change the dimensions of the peel zone.

CONCLUSIONS

A tape peeling model based on a static geometrical consideration of the peel zone was derived which incorporates the role of friction (or shear) on adhesion. The proposed model was tested on a model tape and two types of commercially available adhesive tapes to predict the peel force as a function of peel angle. The model accurately predicted the peel behavior for adhesive tapes with backings of high stretch moduli. Adhesive tapes with low stretch moduli are expected to change the shape of the peel zone and thus deviate from the proposed

model. The model was applied to the gecko adhesive system and nicely explains the apparent discrepancies in the magnitudes of the pull-off forces measured in previous experimental studies performed on different hierarchical structures of geckos.

REFERENCES

Autumn, K., Liang, Y. A., Hsien, S. T., Zesch, W., Chan, W. P, Kenny, T. W., Fearing, R., Full, R., (2005): Adhesive force of a single gecko foot-hair *Nature* 405, 681-685.

Autumn, K., Sitti, M., Liang, Y. A., Peattie, A. M., Hansen, W. R., Sponberg, S., Kenny, T. W., Fearing, R., Israelachvili, J. N., Full, R. J., (2002): Evidence of van der Waals adhesion in gecko setae *PNAS* 99, 12252-12256.

Autumn, K., Hsieh, S. T., Dudek, D. M., Chen, J., Chitaphan, C., Full, R. J., (2006a): Dynamics of geckos running vertically *J. Exp. Bio.* 209, 260-272.

Autumn, K., Dittmore, A., Santos, D., Spenko, M., Cutkosky, M., (2006b): Frictional adhesion: a new angle on gecko attachment *J. Exp. Bio.* 209, 3569-3579.

Autumn, K., Majidi, C., Groff, R. E., Dittmore, A., Fearing, R., (2006c): Effective elastic modulus of isolated gecko setal arrays *J. Exp. Bio.* 209, 3558-3568.

Chen, J. J., Peattie, A. M., Autumn, K., Full, R. J., (2006): Differential leg function in a sprawled-posture quadrupedal trotter *J. Exp. Bio.* 209, 249-259.

Ciccotti, M., Giorgini, B., Vallet, D., Barquins, M., (2004): Complex dynamics in the peeling of an adhesive tape *Inter. J. of Adhesion and Adhesives* 24, 143-151.

Créton, C., Leibler, L., (1996): How does tack depend on time of contact and contact pressure *J. Polymer Sci. B Polymer Phys.* 34, 545-554.

Geim, A. K, Dubonos, S. V., Grigorieva, I. V., Novoselov, K. S., Zhukov, A. A., Shapoval, S. Y., (2003): Microfabricated adhesive mimicking gecko foot-hair *Nature Materials* 2, 461-463.

Gent, A. N., Kaang, S. Y., (1987): Effect of Peel Angle upon Peel Force *J. Adhesion* 24, 173-181.

Hansen, W., Autumn, K., (2005): Evidence for self-cleaning in gecko setae *PNAS* 102, 385-389.

Huber, G., Gorb, S. N., Spolenak, R., Arzt, E., (2005): Resolving the nanoscale adhesion of individual gecko spatulae by atomic force microscopy *Biology Letters* 1, 2-4.

Israelachvili, J.N., *Intermolecular & Surface Forces*, (Elsevier Academic Press, San Diego, 2005). 2nd ed., Chap. 11, pp. 176-179.

Kendall K., (1975): Thin-film peeling-the elastic term *J. Phys. D Appl. Phys.* 8, 1449-1452.

Kinloch, A. J., Lau, C. C., Williams, J. G., (1994): The peeling of flexible laminates *Inter. J. of Fracture* 66, 45-70.

Lindner, A., Maevis, T., Brummer, R., Luhmann, B., Creton, C., (2004): Subcritical Failure of Soft Acrylics under Tensile Stress *Langmuir* 20, 9156-9169.

Newby, B.Z., Chaudhury, M. K., (1998): Friction in Adhesion *Langmuir* 14, 4865-4872.

Northen, M. T., Turner, K. L., (2005): A batch fabricated biomimetic dry adhesive *Nanotechnology* 16, 1159-1166.

Persson, B. N. J., Gorb, S., (2003): The effect of surface roughness on the adhesion of elastic plates with application to biological systems *J. of Chem. Phys.* 119, 11437-11444.

Plaut, R., Ritchie, J., (2004): Analytical Solutions For Peeling Using Beam-on-foundation model and cohesive zone *J. Adhesion* 80, 313-331.

Portigliatti, M., Koutsos, V., Hervet, H., Léger, L., (2000): Adhesion and Defromation of a Single Latex Particle *Langmuir* 16, 6374-6376.

Rivlin R. S., (1944): *Paint Technology* 9, 215.

Ruibal, R., Ernst, V., (1965): Structure of digital setae of lizards *J. Morphology* 117, 271.

Sato, K., Toda, A., (2004): Modeling of the Peeling Process of Pressure-sensitive Adhesive Tapes with the combination of Maxwell Elements *J. Phys. Soc. Jpn* 73, 2135-2141.

Shull, K. R., Creton, C., (2004): Deformation Behavior of Thin, Compliant Layers Under Tensile Loading Conditions *J. Polymer Sci. B Polymer Phys.* 42, 4023-4043.

Spolenak, R., Gorb, S., Gao, H. J., Arzt, E., (2004): Effect of contact shape on the scaling of biological attachments *Proc. R. Soc. Lond. Ser. A Math. Phys. Eng. Sci.* 461, 305-319.

Sun, Z., Wan, K., Dilliard, D. A., (2004): A theoretical and numerical study of thin film delamination using the pull-off test *Inter. J. of Solids and Structures* 41, 717-730.

Tian, Y., Pesika, N.S., Zeng, H., Rosenberg, K., Zhao, B., McGuiggan, P., Autumn, K., Israelachvili, J., (2006, submitted): Adhesion and friction in gecko toe attachment and detachments *PNAS* (2006, submitted)

Wan, K., (1999): Fracture Mechanics of a V-peel Adhesion Test – Transition from a Bending Plate to a Stretching Membrane *J. Adhesion* 70, 197-207.

Williams, J. A., Kauzlarich, J. J., (2005): The influence of peel angle on the mechanics of peeling flexible adherends with arbitrary load-extension characteristics *Tribology International* 38, 951-958.

Yao, H, Gao, H., (2006): Mechanics of robust and releasable adhesion in biology: Bottom-up designed hierarchical structures of gecko *J. of the Mechanics and Physics of Solids* 54, 1120-1146.

Zosel, A., (1998): The effect of fibrillation on the tack of pressure sensitive adhesives *Int. J. of Adhesion and Adhesives* 18, 265-271.

Zosel, A., (1989): Adhesive Failure and Deformation Behaviour of Polymers *J. Adhesion* 30, 135-149.

# Peel Zone Model of Tape Peeling based on the Gecko Adhesive System

Noshir S. Pesika[1], Yu Tian[1], Boxin Zhao[1], Kenny Rosenberg[1], Hongbo Zeng[1], Patricia McGuiggan[1], Kellar Autumn[2], Jacob N. Israelachvili[1]

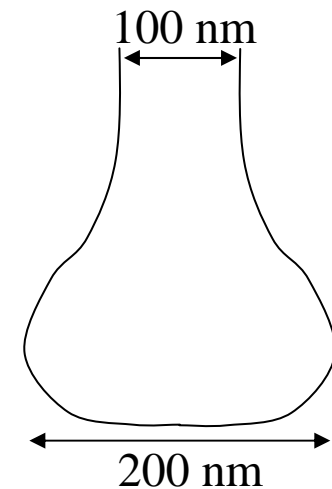[1]Department of Chemical Engineering, University of California
[2]Department of Biology, Lewis and Clark College

The hierarchical structure of the Gecko

Lamella

Setal array

Spatula pads
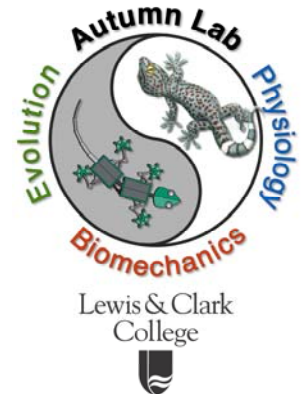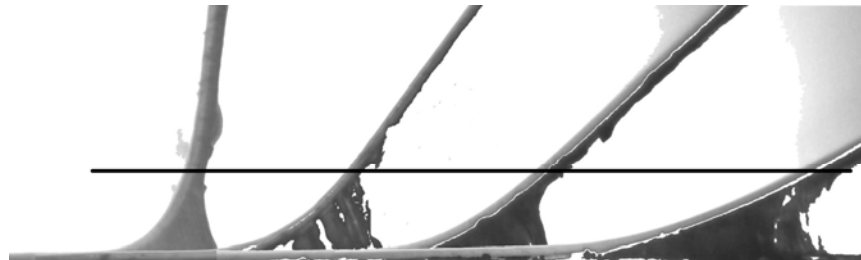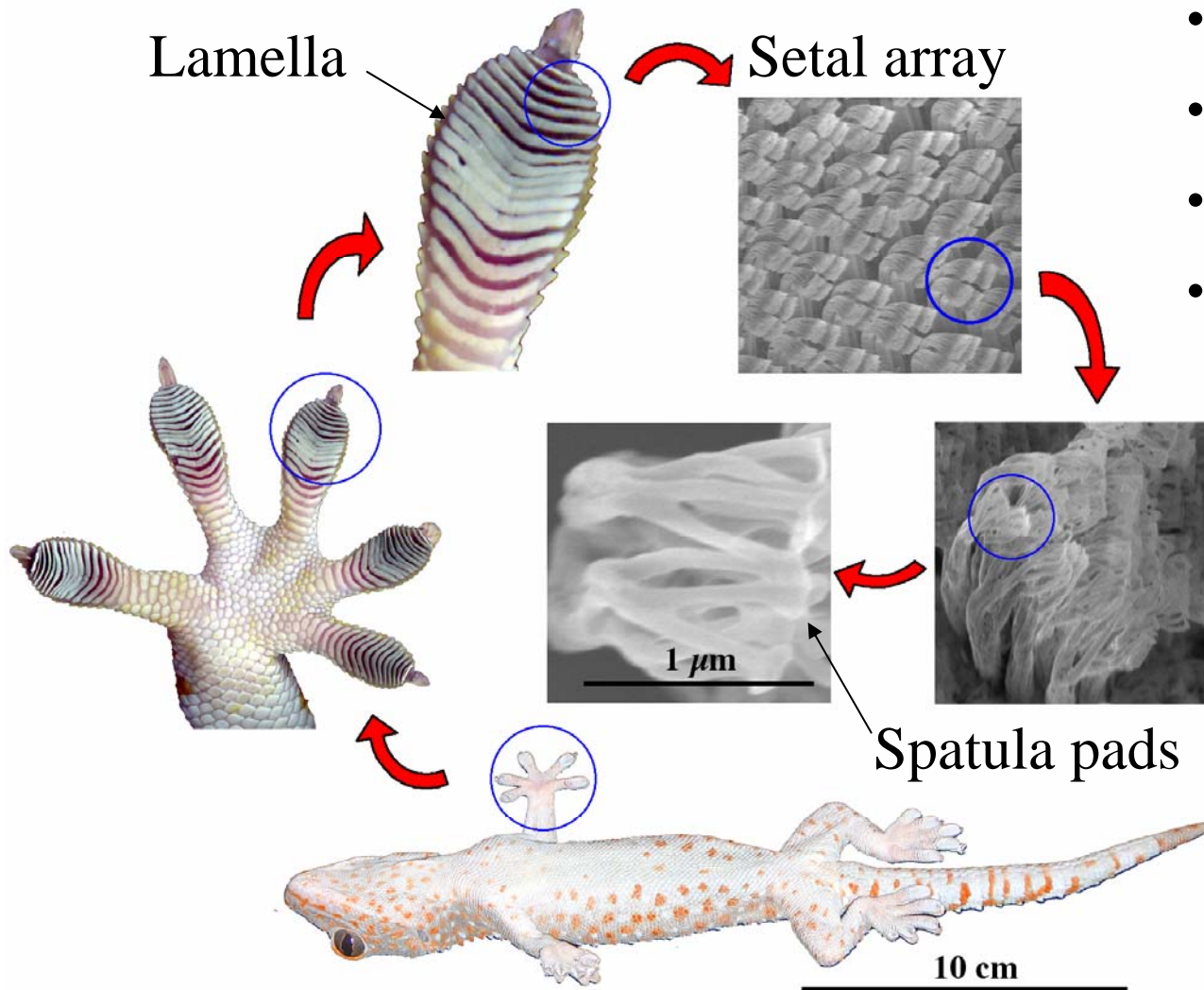
- Compliant structure

- ~14,400 setae/mm^2

- ~40 μN per setae

- Spatula

  - 200 nm wide β-keratin structures narrowing to 100 nm, 10 nm thick

100 nm

200 nm

1 μm

10 cm

Why is the Gecko Adhesive system of interest?

Properties of the Gecko Adhesive system

1. Directional
2. Attaches strongly with minimal preload
3. Detaches quickly and easily
4. Sticks to almost any material (different surface energies, roughness)
5. Remains clean (self-cleaning ability)
6. Does not self-adhere

Potential applications

Reversibly sticky pads on robotic appendage, sticky gloves

What role does geometry play?

Interplay between *Friction* and *Adhesion*

"Y-configuration"
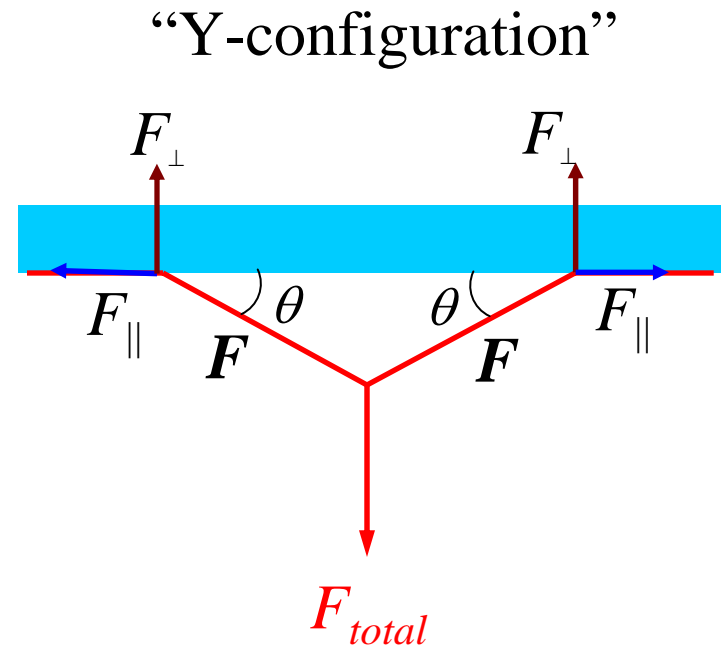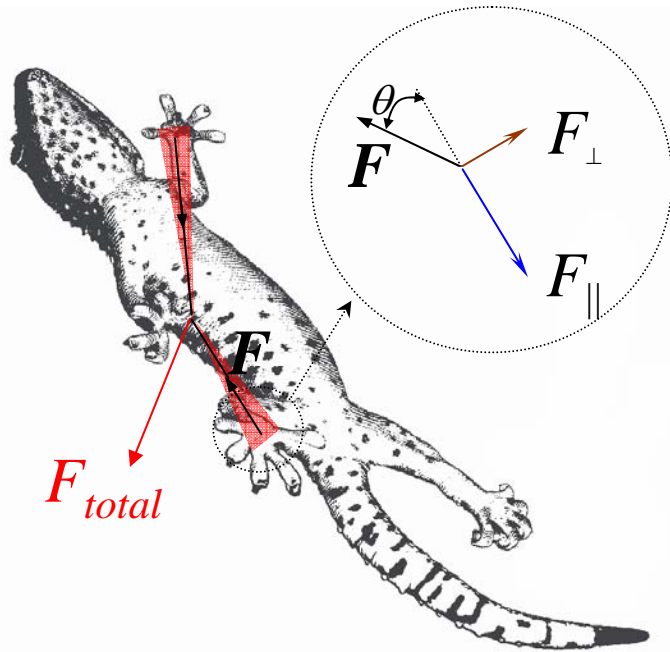
- van der Waals forces
- Relatively weak force

$$F_\perp = \frac{A\, C_{surface}}{6\pi D^3}$$

$$\boldsymbol{F} = F_\perp \sin\theta + F_\parallel \cos\theta$$

Gecko spatula compared to adhesive tape
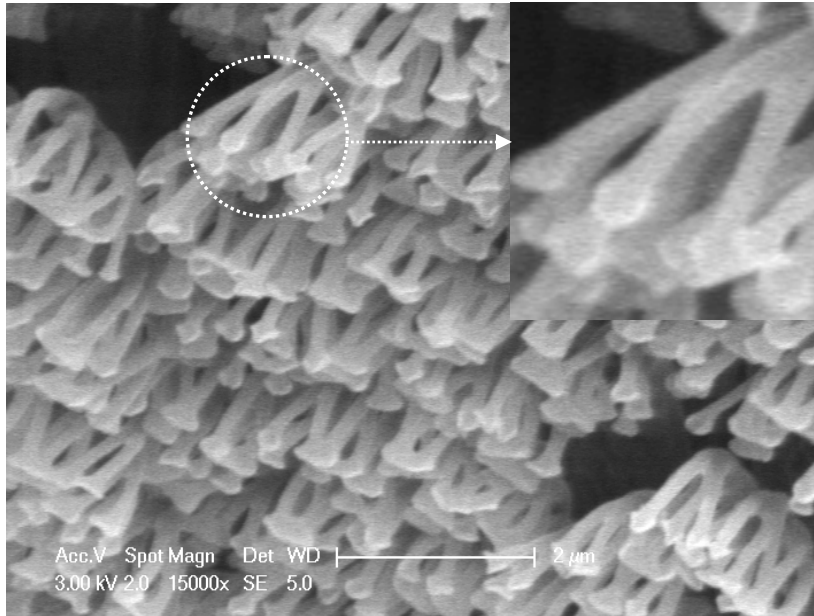
Similarities
- shape, stiffness

Difference
- van der Waals forces instead of viscoelastic filaments
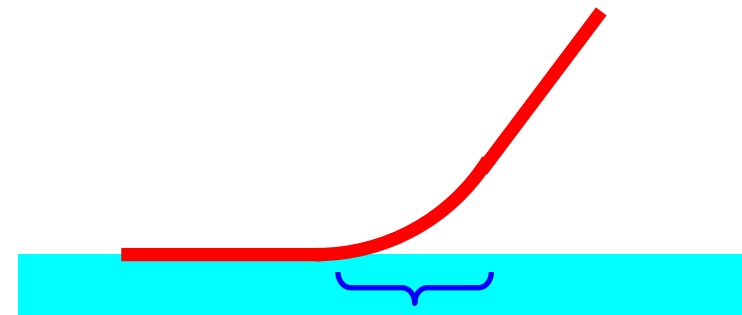
Interaction zone

Tape Peeling Experimental set-up

L-configuration
width b
v
θ
$F_{\perp}$
$F_{\parallel}$
peel zone
γ
θ
F
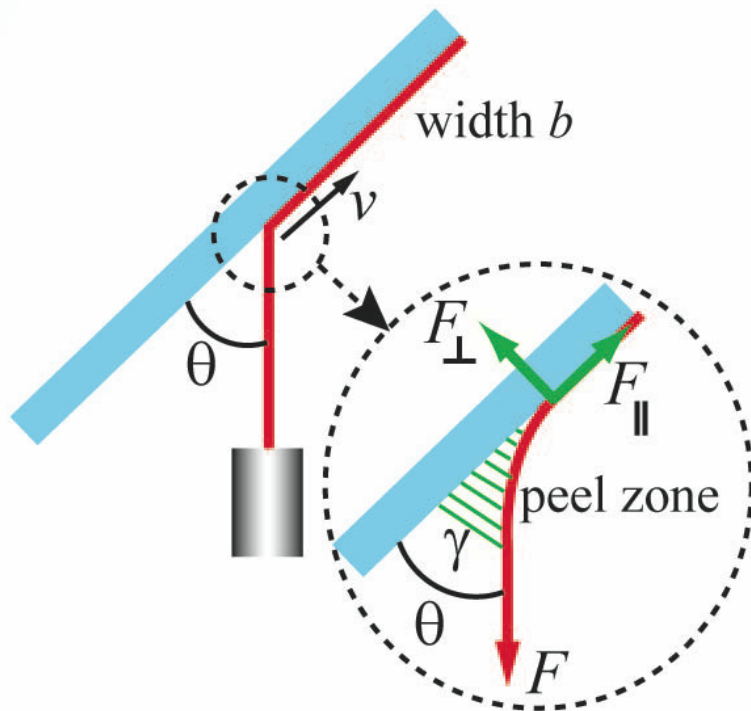
- Tape allowed to adhere for 4 hrs prior to peeling experiment

- Borosilicate (glass) surface tilted to desired angle

- Weight is added until tape peels at constant velocity

- Videos of the peeling process is recorded

- Peel force data at different peel angles is collected

Peel Zone Model

Peel Zone

Peel Zone Model

- Based on a force balance

- Assumptions:
  - Backing has a circular curvature

  - The stationary point remains at a constant distance from the surface

  - Tape backing has a high stretch modulus (i.e., does not stretch)
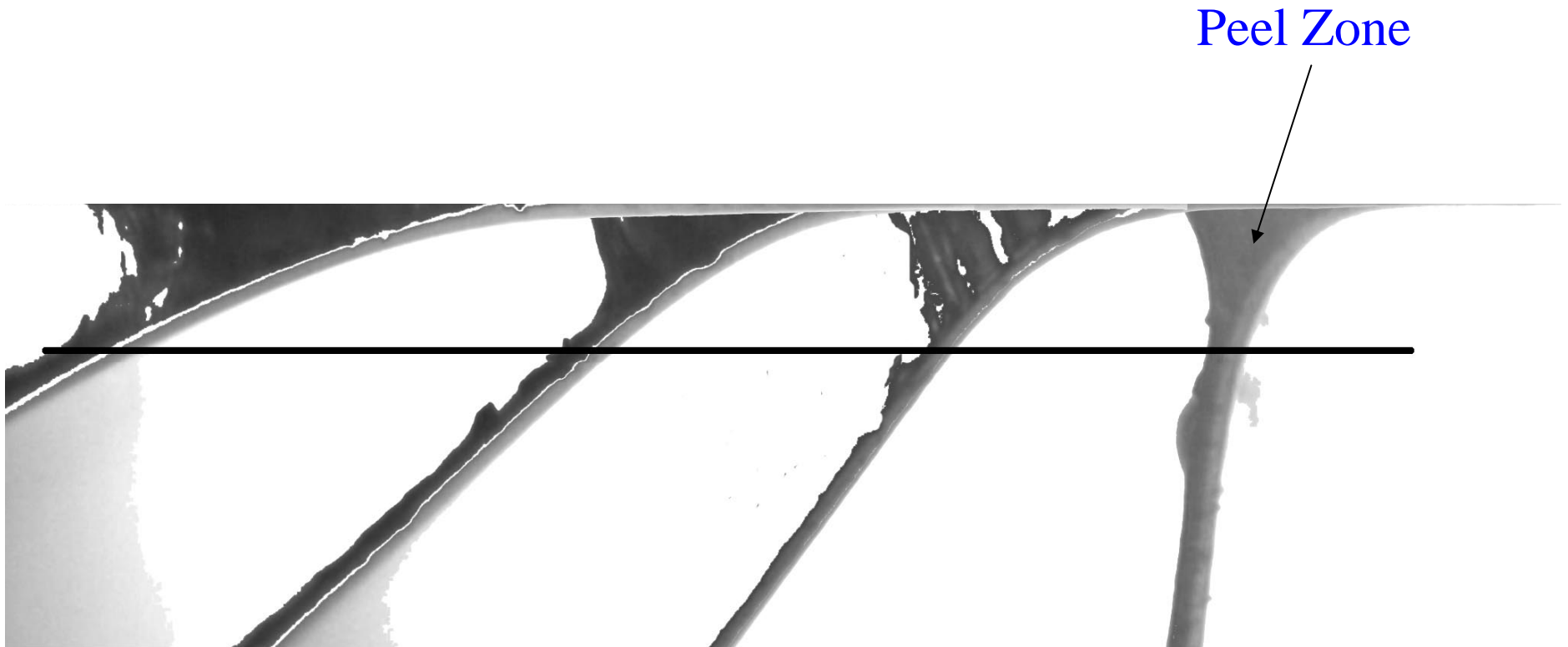
$$\frac{F}{b} = \gamma \left[\frac{\theta}{\phi_o} \right] \left[\frac{1-\cos\phi_o}{1-\cos\theta} \right] \left[\frac{1}{\sin\theta} \right]$$

Geometrical Predictions of the Peel Zone Model
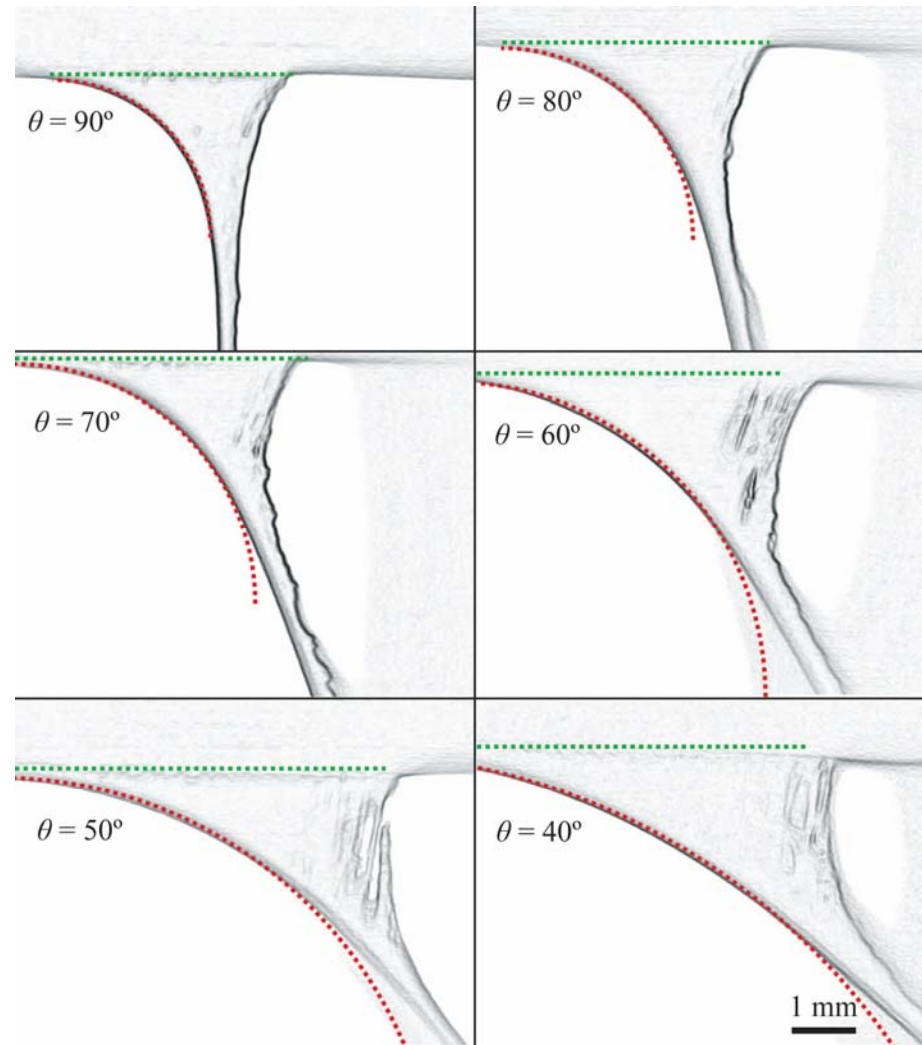
The geometry of the peel zone as predicted by the Peel Zone model is in good agreement with experiments

Peel Force Predictions of the Peel Zone Model

Model tape - double-sided adhesive with transparency backing
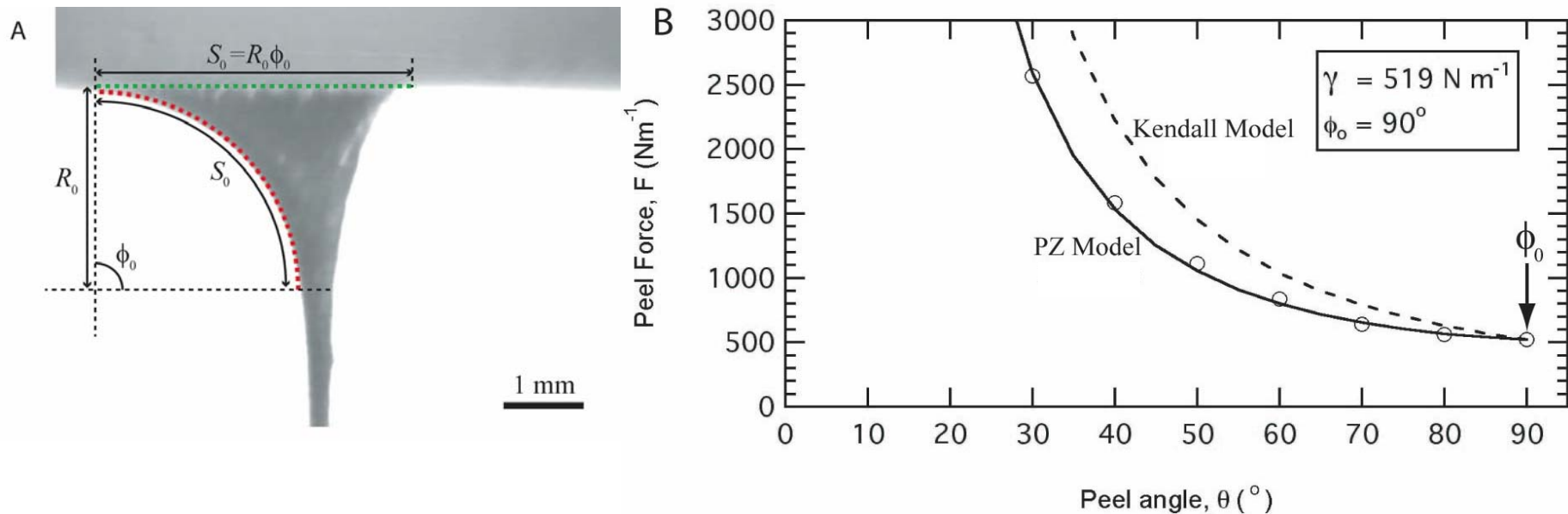
The peel force as a function of the peel angle as predicted by the Peel Zone model is in good agreement with experiments

Peel Force Predictions of the Peel Zone Model

Electrical tape
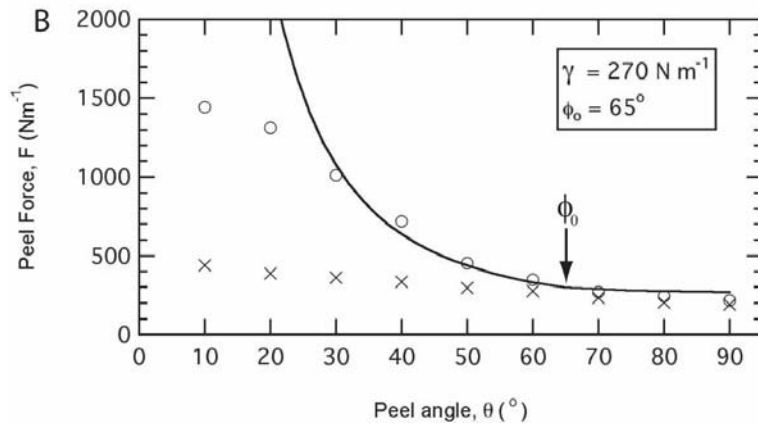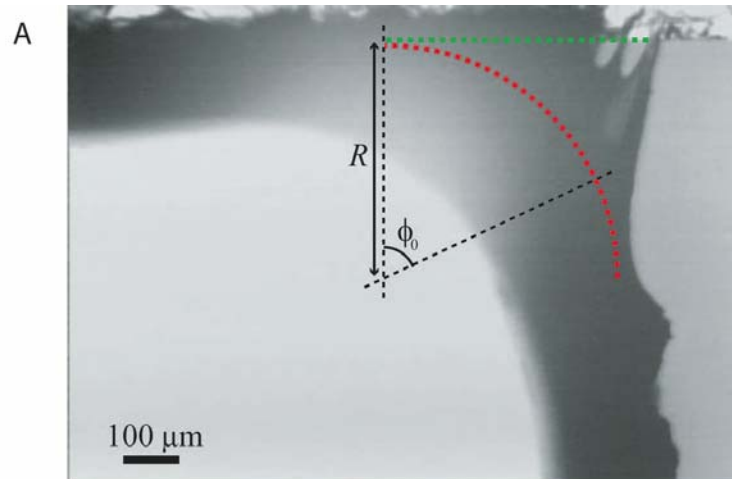
Scotch tape
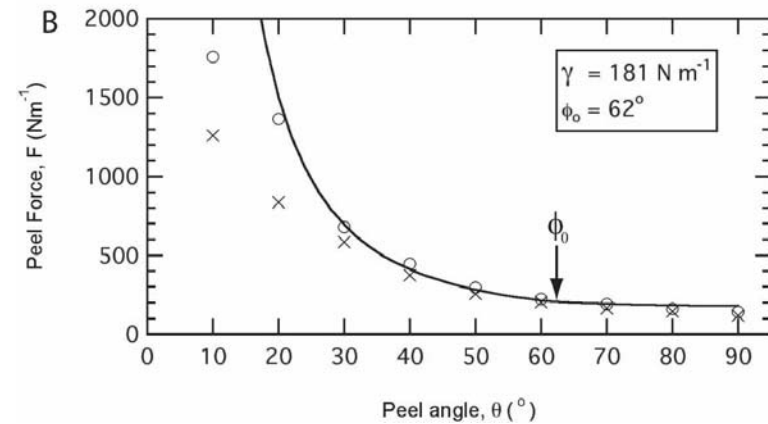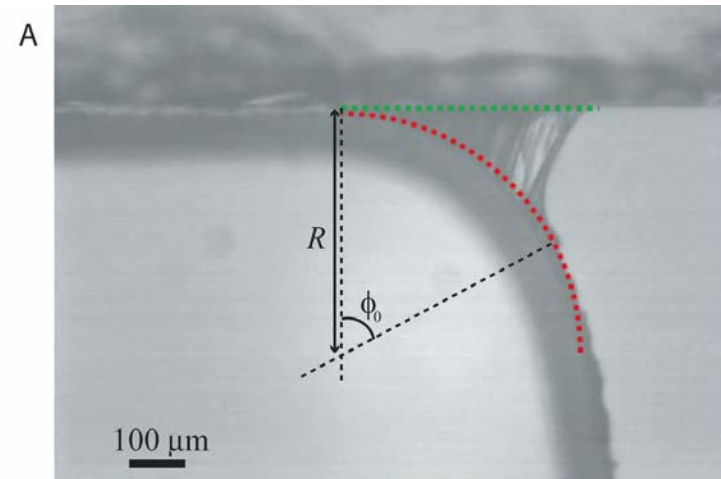
Peel Zone Model applied to a Gecko spatula

Reported values for gecko adhesion

- Huber et al. (2005) - $F_\perp$=10 nN per spatula *or* a Peel Force of 50 mN m^{-1}

- Autumn et al. (2002) - $F_\perp$=40 μN per setae = 40 nN per spatula *or* a Peel Force of 633 mNm^{-1} (assuming 1000 spatulae per setae)
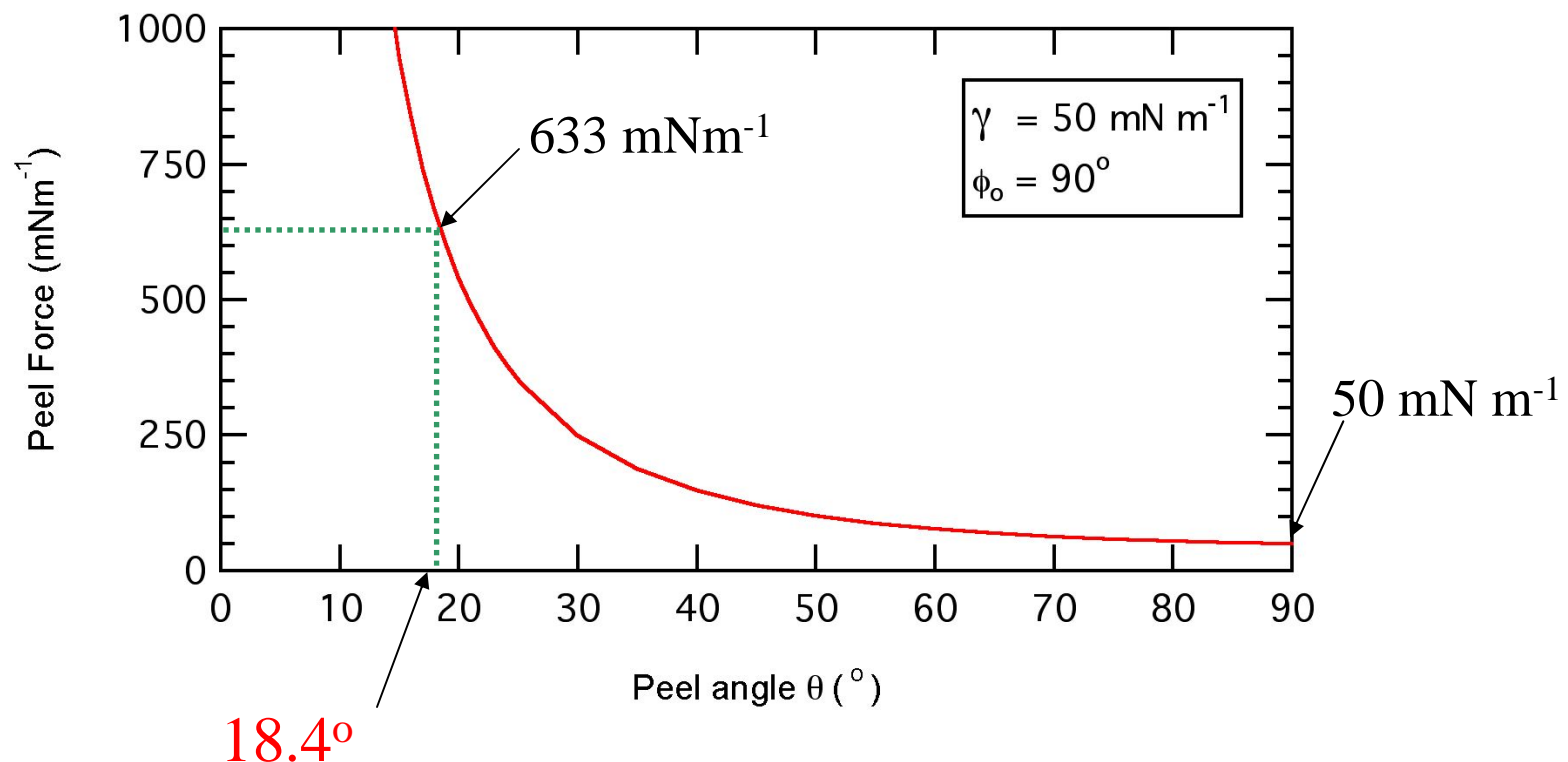
Gecko adhesion - microscopic analysis

$$F_\perp = \frac{A\,C_{surface}}{6\pi D^3}$$

Tian, Y. et al. *PNAS* (in press)

Gecko adhesion - microscopic analysis

Gecko toe Attachment and Detachment
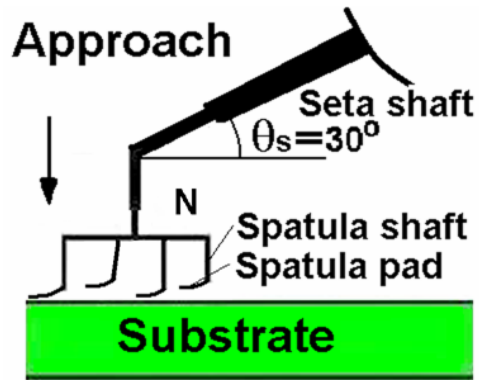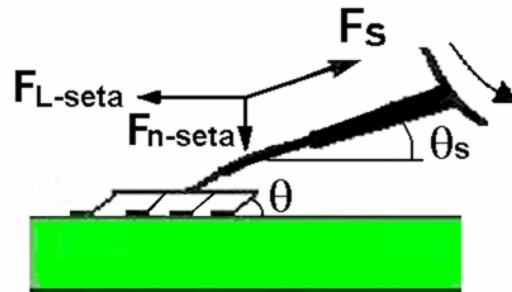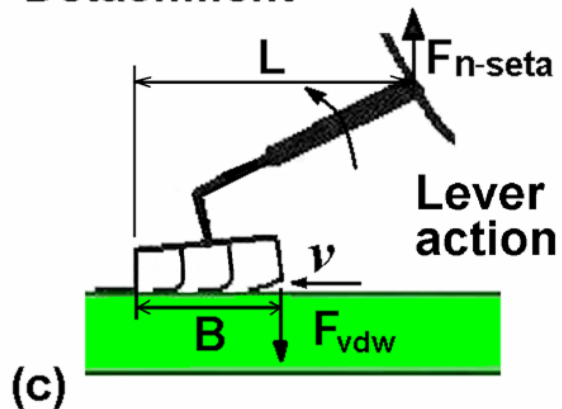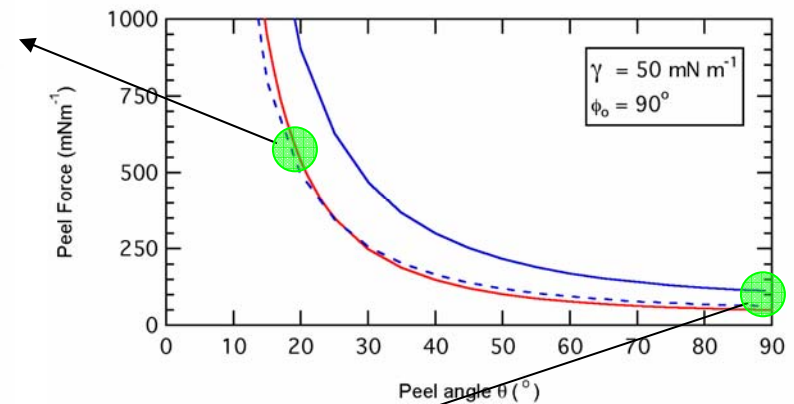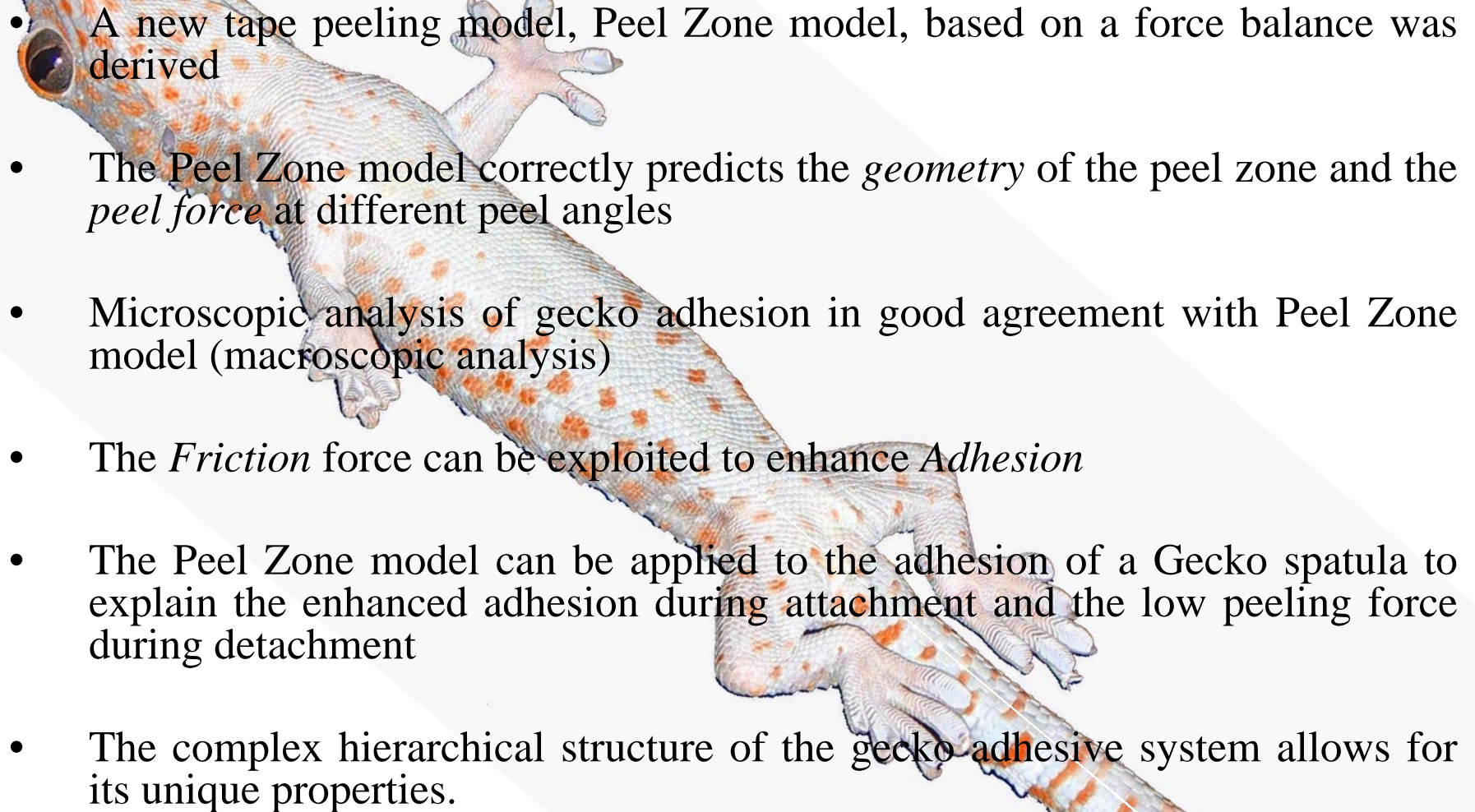

Gecko detachment

Conclusions

- A new tape peeling model, Peel Zone model, based on a force balance was derived

- The Peel Zone model correctly predicts the *geometry* of the peel zone and the *peel force* at different peel angles

- Microscopic analysis of gecko adhesion in good agreement with Peel Zone model (macroscopic analysis)

- The *Friction* force can be exploited to enhance *Adhesion*

- The Peel Zone model can be applied to the adhesion of a Gecko spatula to explain the enhanced adhesion during attachment and the low peeling force during detachment

- The complex hierarchical structure of the gecko adhesive system allows for its unique properties.

Acknowledgement